The interference modulation rate for a band of frequencies which is produced by a constant change in δ may be obtained from (15). It can be seen that the term $1/c(\lambda/\lambda_g)F$ is equal to $\lambda_g{}^*$, where $\lambda_g{}^*$ is the guide wavelength corresponding to the microwave center frequency F. Thus, for uniform change in δ, the microwave power incident upon the detector may be expressed as

$$P_d = \frac{1}{2} kTB \left\{ 1 + \frac{\sin\left[\left(\frac{\omega_a t}{F}\right)\frac{B}{2}\right]}{\left[\left(\frac{\omega_a t}{F}\right)\frac{B}{2}\right]} \cos \omega_a t \right\}. \quad (17)$$

Notice that the magnitude of the periodic peaks caused by a coherent source of power P_s [see (16)] are the same as the peak for an incoherent source [$t=0$ in (17)] for which kTB is equal to P_s.

ACKNOWLEDGMENT

The authors express their appreciation to E. R. Flynt and W. K. Rivers, Jr. for numerous profitable discussions regarding this work. Mr. Rivers introduced the authors to the subject of interference modulation, and Mr. Flynt assisted with many instrumentation problems.

Superheterodyne Radiometers for Use at 70 Gc and 140 Gc*

R. MEREDITH† AND F. L. WARNER†

Summary—In this paper four different millimeter wave equipments, which have been made for plasma diagnostic work, are described. They are:

1) A straightforward 70-Gc superheterodyne radiometer with an over-all noise factor of 13 db;
2) An early 140-Gc radiometer, with second harmonic mixing, which has an over-all noise factor of about 25 db;
3) A later and more sensitive 140-Gc radiometer which contains a fundamental local oscillator, VX 3352 mixer crystals and a 408-Mc IF amplifier commencing with an Adler tube;
4) A very simple 140-Gc transmission measuring equipment containing a 1-watt source and a crystal video receiver which has a tangential sensitivity of −42 dbm.

The last part of this paper discusses the minimum temperature changes which can be detected, at short millimeter wavelengths, with various types of superheterodyne radiometers, the Golay cell, the barretter, the crystal video radiometer, the 1.5°K carbon bolometer and the 1.5°K InSb photoconductive detector. The performances expected from straight traveling-wave tube radiometers and traveling-wave masers at short millimeter wavelengths are also considered.

The Appendices are devoted to mixer crystal performance in the millimeter and submillimeter regions, a theory of second harmonic mixing and the voltage sensitivity of a forward biased detector crystal.

INTRODUCTION

A TOROIDAL shaped fusion machine called ZETA was built at the Atomic Energy Research Establishment (AERE), Harwell a few years ago [1]. The pulses applied to this machine last for a few milliseconds and the electron densities produced in the plasma are in the region of 10^{14} per cm^3. The plasma frequency therefore lies in the gap between the microwave and infrared regions. In 1958, there was some doubt about the value of the temperature being reached inside ZETA and an urgent need arose for sensitive radiometers suitable for making temperature measurements on ZETA in the neighborhood of the plasma frequency.

The Royal Radar Establishment (RRE) was asked to tackle this problem from both the microwave and infrared sides of the gap. This paper describes the extension of superheterodyne radiometer techniques into this part of the spectrum. The outstanding progress made by the RRE infrared team has already been described elsewhere [2]–[5]. Considerable overlapping of radio and infrared techniques has now occurred.

In addition to needing sensitive radiometers at short millimeter wavelengths, a need also arose at AERE for equipments suitable for making transmission and phase shift measurements through plasmas at various wavelengths throughout the millimeter region. One equipment falling into this category is also described in this paper.

THEORETICAL PERFORMANCE OF MIXER CRYSTALS IN THE MILLIMETER AND SUBMILLIMETER REGIONS

At short millimeter wavelengths, the performance of a superheterodyne radiometer is mainly determined by the mixer crystals, so four years ago an attempt was made to work out the over-all noise factors which it should be possible to obtain with silicon, germanium and gallium arsenide mixer crystals, over the wavelength

* Received January 21, 1963.
† Royal Radar Establishment, Great Malvern, Worcs. England.

range 10 cm to 0.1 mm. These calculations were based upon the theoretical work and data published by Torrey and Whitmer [6], Southworth [7], Sharpless [8], Messenger and McCoy [9] and Jenny [10]. The results obtained are presented in Fig. 1 and Appendix I gives the theoretical expressions and data which were used. These curves provided a source of encouragement for us at the outset of this work and further reference will be made to them later on.

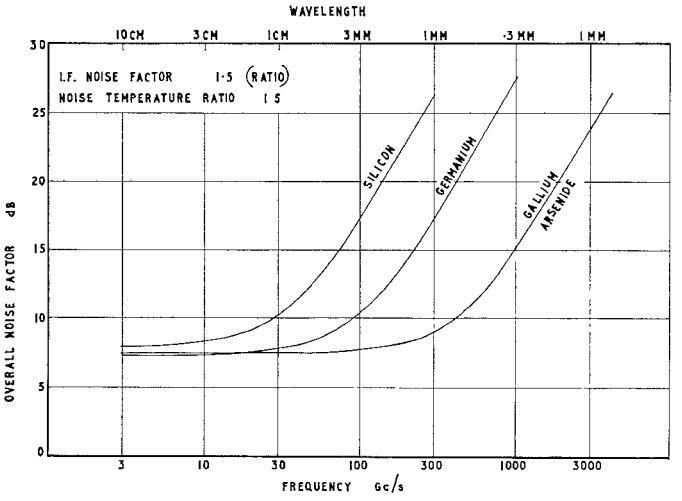

Fig. 1—Theoretical curves of over-all noise factor vs frequency for silicon, germanium and gallium arsenide mixer crystals.

70-Gc Superheterodyne Radiometer

In 1959, a 70-Gc superheterodyne radiometer was made for A.E.R.E.; and during the last three years it has been used, successfully, on many occasions for making temperature measurements on ZETA and various other plasma generators. Simplified block diagrams of this radiometer are shown in Fig. 2. The upper block diagram shows how it is connected up for temperature measurements on ZETA. In this case, the equipment takes the form of a straightforward superheterodyne receiver. A Philips DX 151 4.3-mm reflex klystron [11] is used as local oscillator and two Philco IN2792 germanium diodes are employed in the balanced mixer. The IF amplifier has a bandwidth of 10 Mc centered on 45 Mc, and the second detector is followed by a simple low pass filter with a time constant short enough to reproduce the ZETA pulses. (A $\frac{1}{4}$-ms time constant is normally used.) The output is displayed on a memoscope.

The 4.3-mm radiation from ZETA is fed through the ferrite switch into the receiver and it gives an output as shown on the right-hand side of Fig. 2. At the end of the plasma pulse the ferrite switch is changed over by a delayed trigger pulse and a reference signal is now received from the argon noise tube. The rotary attenuator is progressively adjusted until the plasma and reference signals are of equal amplitude. It is then a straightforward matter to relate the effective temperature of the plasma to the temperature of the argon tube.

If the temperature of the argon tube is not known it has to be determined in some way and the best method is to compare its noise output with that from a well-matched termination at an accurately known temperature. This 4.3-mm radiometer was designed so that it can be changed over in a few seconds to a form in which it is suitable for calibrating noise tubes. Its block diagram is then as shown in the lower part of Fig. 2. A sealed waveguide termination immersed in boiling water is used as a standard noise source, and, to obtain an accurate balance, the radiometer sensitivity is greatly increased by using a much narrower output bandwidth than in the previous case. Gain variation noise is eliminated by switching between the two input sources at 20 cps and then converting the amplified 20-cps signal back to dc with a phase sensitive detector. The rotary attenuator is adjusted until the radiometer output is zero and calculation of the argon tube tempeature is then straightforward.

In each case, "equal input" techniques are used so the results are not affected by the law of the radiometer and they are not affected by slow gain variations in the amplifiers. A photograph of this radiometer is shown in Fig. 3.

Several pairs of IN2792 diodes, which were tested in this equipment, gave over-all noise factors in the region of 13 db. The lowest noise factor measured was 11.8 db. (All the noise factors quoted in this paper are single channel noise factors and they are 3 db higher than the radiometer noise factors quoted by some workers.)

The second recording in Fig. 4 (page 400) was obtained by immersing the input termination of this radiometer in boiling water. A coherent detector time constant of 1 second was used and the output noise is seen to correspond to a peak-to-peak temperature fluctuation of about 6°C. For comparison purposes, one of the best recordings obtained with an 8.6-mm radiometer, containing CV 239/2 mixer crystals, is shown at the top of Fig. 4. In this case the input termination was immersed in melting ice and the coherent detector time constant used was again 1 second.

In a millimeter wave superheterodyne radiometer with mechanical modulation, as described by Dicke [12] it is well known that 1) reflected local oscillator noise, 2) the dependence of IF impedance on RF impedance, and 3) reflected local oscillator power can give rise to large spurious signals unless the chopping disk and input guide are perfectly matched. To reduce these spurious signals, it has now become standard practice to insert a ferrite isolator between the mechanical modulator and the mixer. However, the type of $\pm 45°$ ferrite structure used in this 70-Gc radiometer combines the functions of an isolator and a switch because any spurious signal originating in the receiver has to pass through the ferrite structure twice before it can cause any harm. In doing so it suffers a total rotation of 90° and is absorbed in the resistive vane. However, during the change-over periods

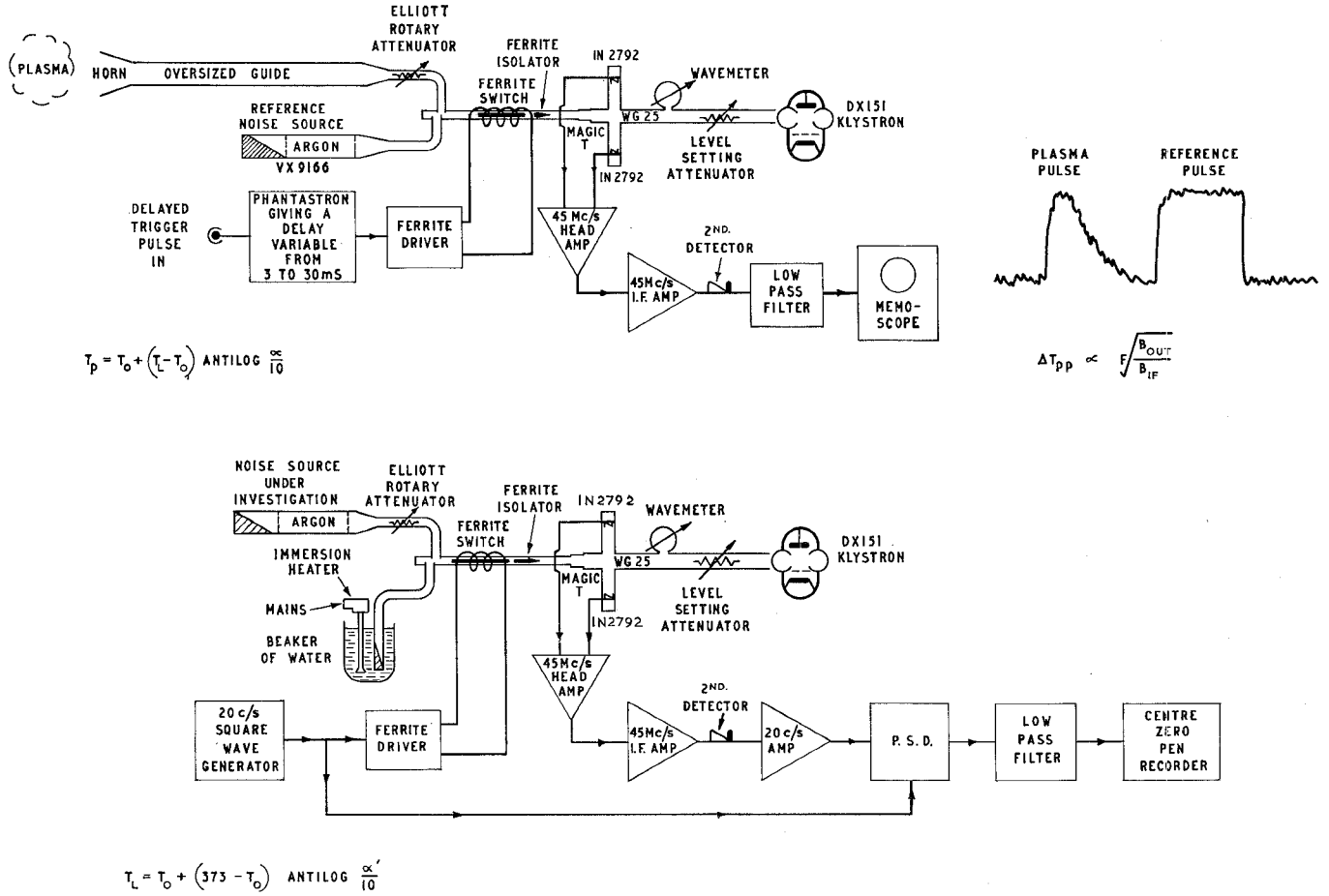

Fig. 2—Simplified block diagrams of the 70-Gc superheterodyne radiometer.

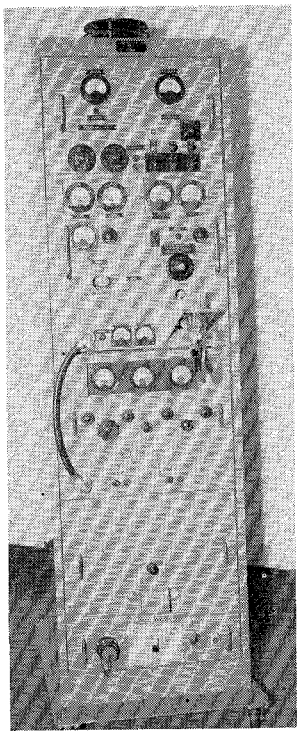

Fig. 3—Photograph of the 70-Gc superheterodyne radiometer.

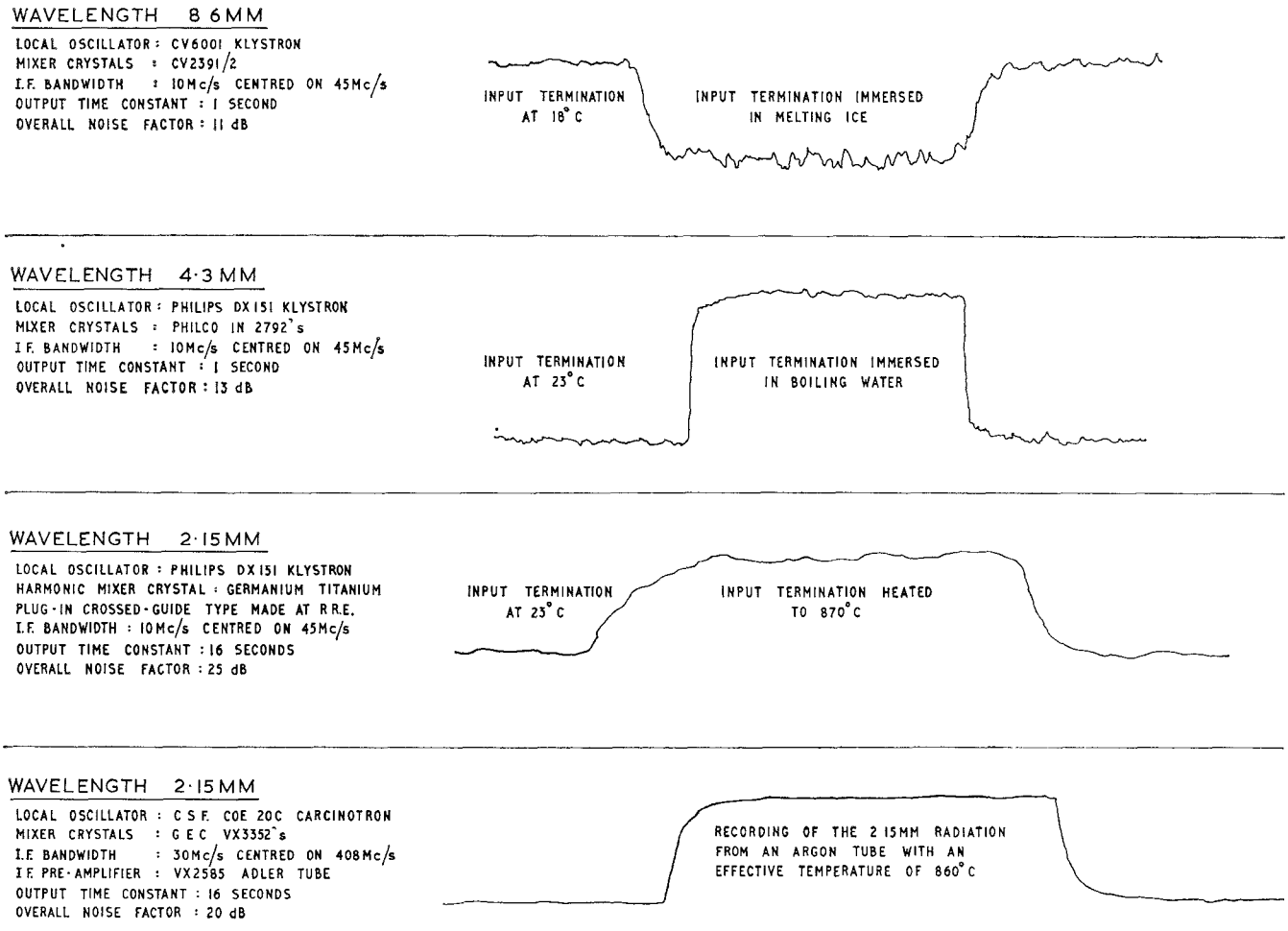

Fig. 4—Radiometer calibration signals at wavelengths of 8.6, 4.3 and 2.15 mm.

of the switch, when the total rotation changes from $+90°$ to $-90°$, small spurious spikes occur; so an isolator has also been included in this 70-Gc radiometer. The two ferrite components together reduce the spurious signals to an undetectable level, even when a shorting piston is connected to one of the input waveguides and moved through several wavelengths.

The effective 4.3 temperature of the VX 9166 argon tube built into this radiometer was found to be 6500°K.

The spreading resistances of the eleven available IN2792 diodes were found to lie in the range 15 to 23 ohms. Their barrier capacitances were estimated from both conversion loss and voltage sensitivity measurements at 70 Gc. Under optimum mixing conditions, the effective values of the barrier capacitances appear to be in the region of 0.06 pf; and the values deduced for the zero-bias capacitances, from voltage sensitivity measurements, are 2 to 3 times lower than this.

140-Gc Superheterodyne Radiometer with Second Harmonic Mixing

In 1960, A.E.R.E. asked for a 2-mm superheterodyne radiometer. At this time, 2-mm fundamental oscillators were not commercially available; so a radiometer employing second harmonic mixing was built. A block diagram of this equipment is shown in Fig. 5 and a photograph of it is shown in Fig. 6.

Due to the lack of a good 2-mm magic T at this time, the mixer was made single ended and a filter cavity was included to eliminate most of the local oscillator noise. With this cavity in use, automatic frequency control (AFC), proved to be essential, and was accomplished very simply by using the well-known frequency-modulation method [13].

The 2-mm temperature of the VX 9166 argon tube was found to be below 1000°C, so in this radiometer the reference signals are obtained from a saturated tungsten diode which is pulsed on at the appropriate times and has its output injected into the first stage of the IF amplifier. An advantage of this arrangement is that the entire plasma signal can now be fed into the mixer but it is now necessary to calibrate the equipment more often as the conversion loss of the mixer is no longer included in the null detection system. Fortunately, in practice, the conversion loss of the harmonic mixer crystal seems to stay surprisingly constant.

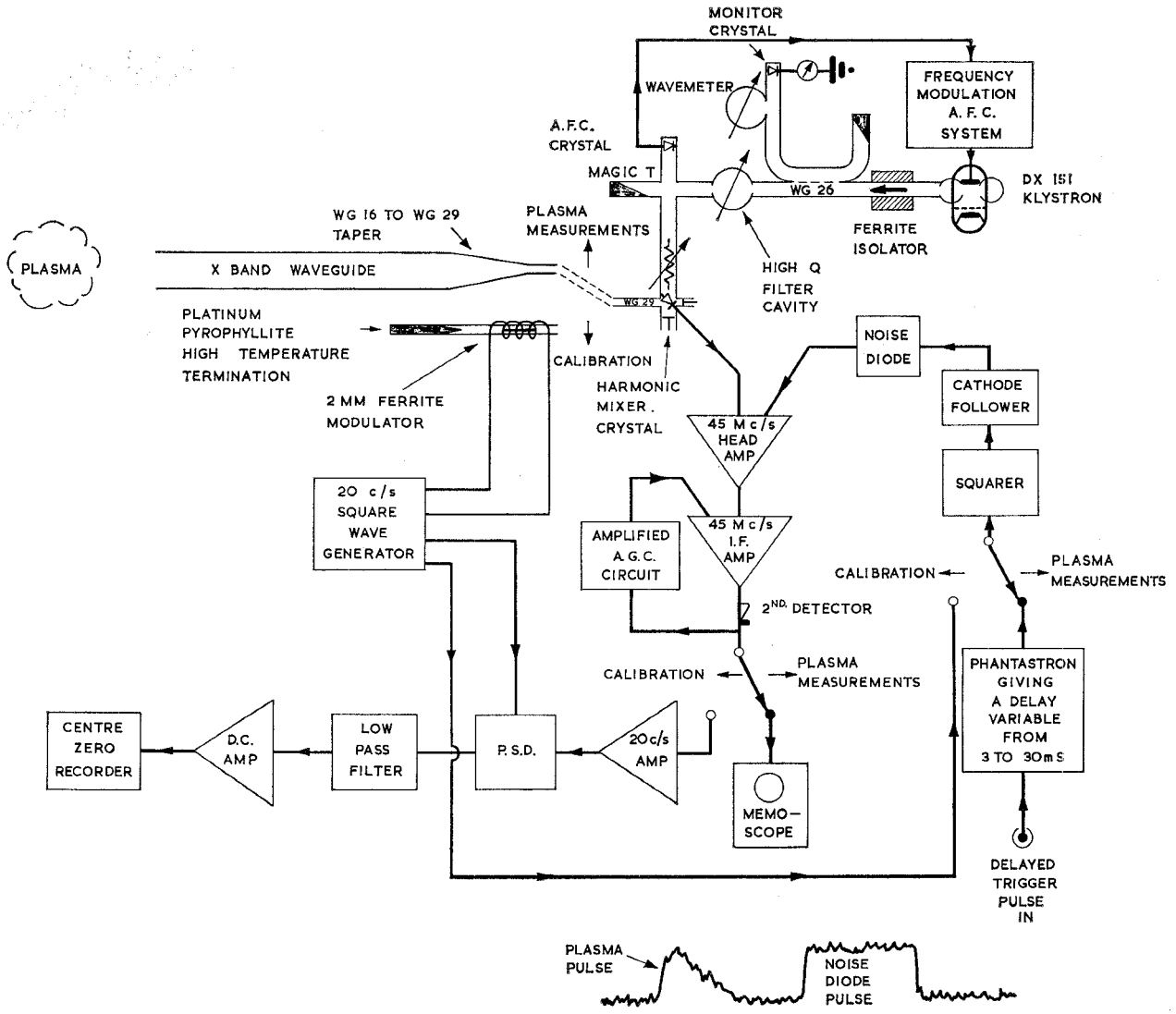

Fig. 5—Block diagram of the 140-Gc radiometer with harmonic mixing.

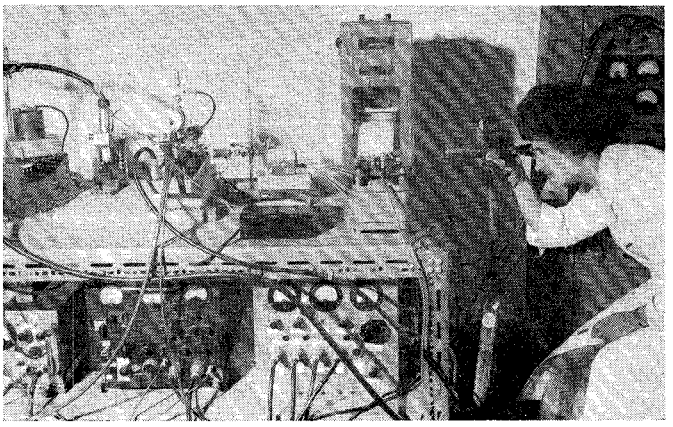

Fig. 6—Photograph of the 140-Gc radiometer with harmonic mixing.

For a harmonic mixer radiometer it should be noted that only four waveguide components have to be developed for use at the signal frequency. These are a waveguide taper, a hot termination, an amplitude modulator and the harmonic mixer.

It is necessary to operate this radiometer about 20 feet away from ZETA; so the 2-mm radiation from the plasma is transmitted over this distance in X-band waveguide and then passed through a long X band to 2-mm taper which was made by electroforming onto a lucite mandrel.

The 2-mm high temperature termination was developed by Q. V. Davis of R.R.E. It contains a rod of pyrophyllite with a conical end. This is held in a TE_{11} circular waveguide formed by a sheet of platinum bent as shown in Fig. 7. The two ends of this platinum sheet are insulated from each other by a sheet of mica. This termination is heated by passing about 500 amperes through the platinum sheet. It can be operated successfully at temperatures up to the softening point of mica. The temperature is kept uniform with surrounding asbestos blocks and it is measured by looking at the end of the pyrophyllite rod with an optical pyrometer (see Fig. 6).

In the early work on this radiometer, a 2-mm mechanical waveguide modulator similar to that described by Dicke [12] was used, but this introduced synchronous microphony, so it was replaced by a 2-mm Faraday rotation amplitude modulator with an "on" loss of 2 db and an "off" loss of 30 db.

It was felt that it would be both interesting and necessary to experiment with several different harmonic mixer crystals; so, inspired by the work of Ditchfield [14], they were assembled in crossed-guide plug-in units. One of these is shown in Fig. 8 together with the associated holder. These plug-in units were made by a copper-gold eutectic process which has been described elsewhere [15]. The lower part of each plug-in unit has been made removable so that the whisker can be replaced easily. The crimp is positioned so that it comes in the 4-mm waveguide and the straight end of the whisker passes through a small hole into the 2-mm waveguide where it makes contact with the semiconductor. Several silicon, germanium and gallium arsenide harmonic mixer crystals were assembled at RRE and tried out in this radiometer. All the silicon ones gave over-all noise factors in excess of 30 db but a fair percentage of the germanium and gallium arsenide ones gave over-all noise factors in the region of 25 db.

The third recording shown in Fig. 4 was obtained, with this radiometer by heating up the platinum pyrophyllite termination to 870°C. The coherent detector time constant used in this case was 16 seconds.

Although an over-all noise factor of 25 db must sound very high to people working at centimeter wavelengths, nevertheless the 2-mm temperature of ZETA was successfully measured, with this radiometer, under a wide variety of operating conditions in December, 1960; and the results obtained were in reasonable agreement with the temperatures deduced from far-infrared measurements on ZETA. In the following year, AERE used this equipment to measure the solar temperature and the atmospheric attenuation at a wavelength of 2 mm [16].

When each harmonic mixer crystal was being tested, the local oscillator drive was varied to obtain the optimum noise factor and it was found, much to our surprise, that the optimum value for the crystal current

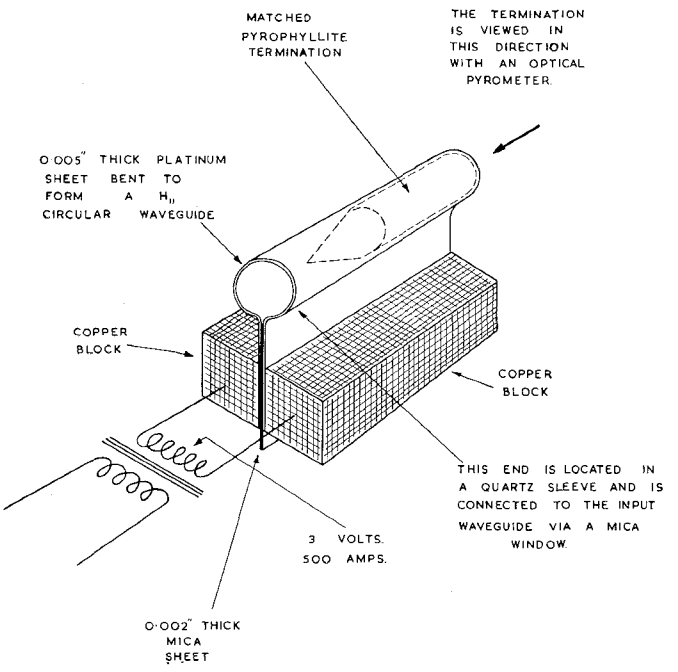

Fig. 7—Diagram of the 2-mm high temperature termination.

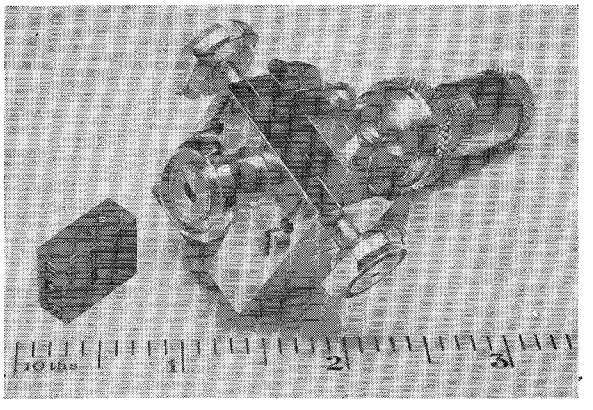

Fig. 8—Photograph of a cross-guide plug-in harmonic mixer crystal and the associated holder.

was never greater than 0.5 ma and, on average, it was significantly lower than the optimum crystal current for fundamental mixing.

There appear to be few references to harmonic mixing in the literature [6], [17]–[19] and no full theory has been found, so an attempt has been made to work out an approximate theory for second harmonic mixing and this is given in Appendix II. When both spreading resistance and barrier capacitance are neglected, this theory yields the dotted curves shown in Fig. 9. For comparison purposes, the corresponding curves for fundamental mixing are also shown in this figure. These were calculated using the appropriate equations from Torrey and Whitmer [6], The noise-temperature ratio and crystal current curves in Fig. 9 are common to both types of mixing. Perfect matching was assumed when calculating the two conversion loss curves shown in this figure, but when working out the over-all noise factor curves, the internal resistance of the signal source was assumed to have a constant value of 500 ohms and the mismatch loss was taken into account. The interesting features emerging from this analysis are:

1) The minimum over-all noise factor with second harmonic mixing is not very much worse than that obtained with fundamental mixing;
2) the optimum value for the local oscillator voltage is lower for second harmonic mixing than it is for fundamental mixing.

Both of these features are in agreement with our experimental results.

When one of the best germanium crystals was in use and giving an over-all noise factor of 25 db, as many parameters as possible were measured. The IF noise factor was found to be 1.8, the crystal noise temperature ratio was 1.8 with $\frac{1}{2}$ ma of crystal current and the excess noise temperature ratio due to local oscillator noise was found to be 2.8 at $\frac{1}{2}$ ma due to an inadequate Q in the filter cavity. The combined loss due to IF amplifier, crystal and local oscillator noise under these circumstances is plotted against the local oscillator voltage in Fig. 10 and this figure also includes the low-frequency conversion loss curve for second harmonic mixing. The spreading resistance, r, of this particular crystal was found from dc measurements to be about 20 ohms, and its barrier capacitance, C, under mixing conditions must be similar to that in IN2792 diodes, so the curve giving the loss due to C and r was calculated for $r=20$ ohms and $C=0.06$ pf. The curve giving over-all noise factor is the sum of these other three curves and it is seen to pass through a minimum value of 24 db, which is in surprisingly good agreement with the measured value of 25 db. Under optimum conditions it can be seen that the spreading resistance and barrier capacitance cause a loss of about 9 db and the loss due to IF amplifier, crystal and local oscillator noise is also about 9 db.

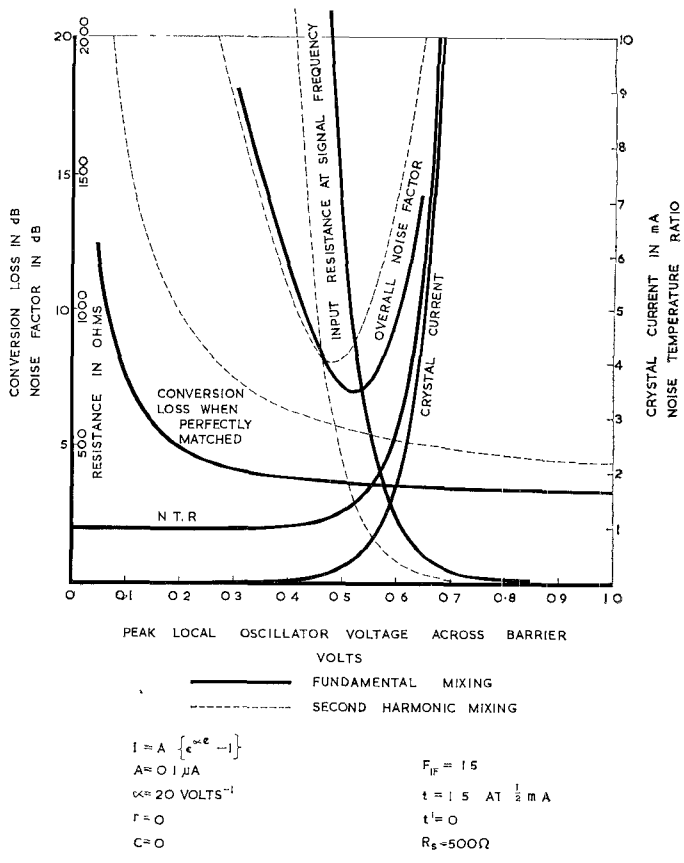

Fig. 9—Theoretical curves for fundamental and second harmonic mixing when both spreading resistance and barrier capacitance are neglected.

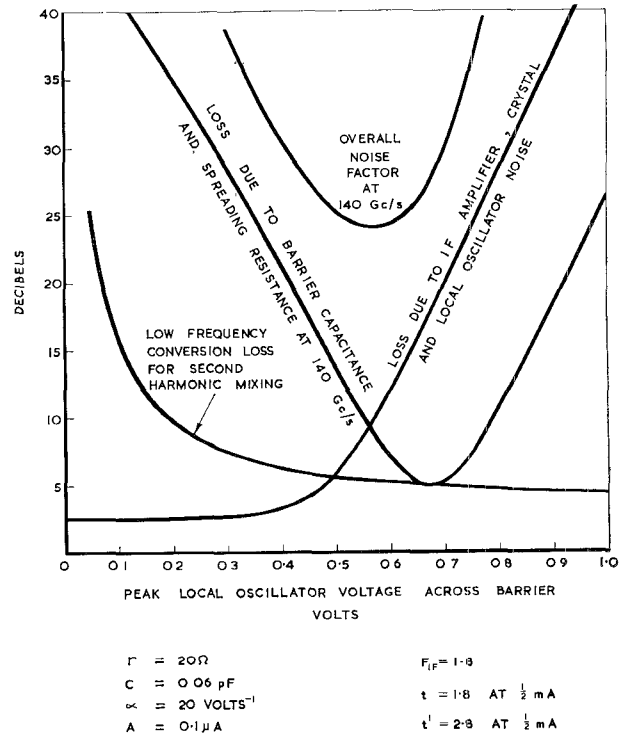

Fig. 10—Performance curves for the 140-Gc radiometer with harmonic mixing.

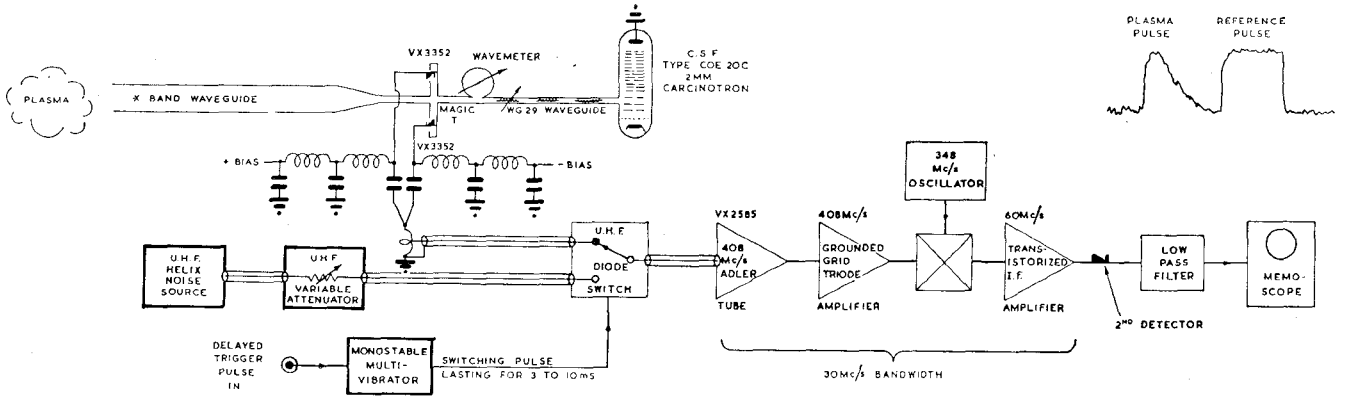

Fig. 11—Simplified block diagram of the 140-Gc superheterodyne radiometer with fundamental mixing.

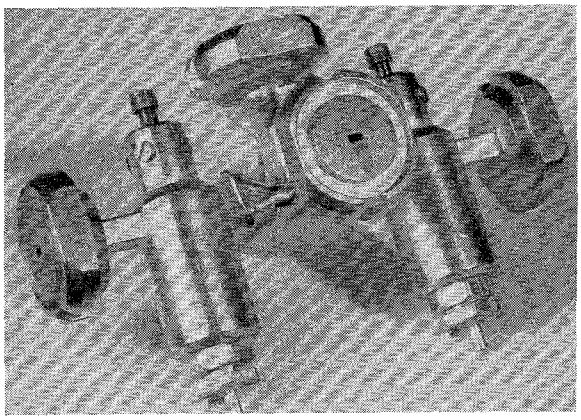

Fig. 12—Photograph of the 2-mm integrated balanced mixer.

140-Gc Radiometer with Fundamental Mixing

In 1961, the Compagnie générale de télégraphie Sans Fil (C.S.F.), announced that they had obtained powers well in excess of 1 watt from 2-mm carcinotrons [20], so work was started at R.R.E. on an improved 140-Gc radiometer with one of these C.S.F. carcinotrons as the local oscillator. The block diagram in Fig. 21 shows how this new 140-Gc radiometer is arranged for plasma measurements. Since the performance of the 140-Gc radiometer described in the previous section was seriously degraded by local oscillator noise, an attempt has been made in this new radiometer to eliminate the deleterious effects of local oscillator noise by using a balanced mixer and centering the early stages of the IF amplifier on 408 Mc. In order to obtain a low IF noise factor with this high intermediate frequency, an Adler tube [21], [22] is used in the first IF stage. The Adler tube appears to be well suited for use as an IF preamplifier in radiometers as it receives broad-band noise from the mixer crystals and this enters both the signal and idler channels. Its noise factor in this application is therefore about 1.5 db instead of the 4.5 db obtained with single channel operation and the idler termination at room temperature.

Oversized waveguide is again used to convey the plasma signal to the radiometer. The mixer crystals are mounted in the side arms of an electroformed 2-mm magic T which has been described elsewhere [15]. A photograph of the integrated balanced mixer is shown in Fig. 12. The mixer crystals are VX 3352 germanium/titanium diodes which were developed by the British General Electric Company, primarily for use at 35 Gc. However, since they are extremely small (0.1 inch in diameter) and are mounted inside low-loss dielectric tubes, they are small enough for use at all wavelengths down to 1 mm. At 140 Gc they give a very good performance and a reasonable match when mounted centrally in standard 0.065 in $\times$ 0.0325 in waveguide. The crystal current can be rapidly optimized by adjusting the axial position and orientation of the diode inside the waveguide and tuning the back plunger. Without bias, diodes of this type have rectification efficiencies at 140 Gc in the region of 150 μa/mw.

The C.S.F. carcinotron, which is used as the local oscillator, is supplied from a highly stabilized power unit which was designed by one of the authors. When it is delivering 150 ma at 6 kv, the output ripple is less than 1-mv peak to peak and a 20-per cent mains variation does not change the output by more than 0.002 per cent.

In this radiometer, the reference signals are obtained from a UHF helix noise source and they are injected into the Adler tube via a UHF attenuator and a UHF diode switch, which is controlled by a triggered monostable multivibrator.

The Adler tube is followed by two lecher line coupled CV2453 grounded grid triode amplifiers and then by an E80CF triode pentode which is used to change the intermediate frequency to 60 Mc. The main IF amplifier contains four 2N1742 transistors with series compensated interstage networks [23]. The entire IF amplifier has an almost flat response over a bandwidth of 30 Mc.

When absolute temperature measurements are required on plasmas, it is necessary to determine the conversion loss in the mixer crystals. This is done by connecting the platinum pyrophyllite termination, described earlier, to the input via a ferrite amplitude modulator and converting the rest of the equipment to a Dicke type radiometer, with 480-cps square-wave modulation. After the signal from the pyrophyllite termination has been recorded, the diode switch is driven at 480 cps and the UHF attenuator is adjusted until a signal of equal amplitude is obtained from the UHF helix noise source.

The bottom recording in Fig. 4 was obtained with this new radiometer when a VX 9166 argon tube with an effective 2-mm temperature of 860°C was connected to the input and switched on. The performance of this new radiometer is seen to be significantly better than that of the 140-Gc radiometer with harmonic mixing. Work on this new radiometer was still in progress at the time of writing but preliminary measurements indicate that it has an over-all noise factor in the region of 20 db. It is hoped to obtain a slightly better noise factor than this with additional refinements.

140-Gc Transmission Measuring Equipment

A very simple 2-mm transmission measuring equipment has recently been made for plasma investigations at A.E.R.E. The transmitter contains a C.S.F. 2-mm carcinotron with a power output of 1 watt and the signal which is picked up by a horn on the opposite side of the plasma is fed straight into a crystal video receiver.

The video amplifier is fully transistorized and is operated from internal batteries. It has a flat response from 1 cps to 1 Mc and a maximum gain of 100 db. It is mounted inside a fully screened chassis, a mumetal box and two $\frac{1}{8}$-in thick copper boxes. Unwanted pickup is completely undetectable when this amplifier is operating only a few feet away from ZETA.

Several silicon, epitaxial silicon and germanium detector crystals have been tested in this receiver and the best results have been obtained with VX 3352 germanium/titanium crystals in a 2-mm holder. Tangential sensitivities of −42 dbm have been achieved with several crystals of this type. Best results are obtained from this receiver by using a forward bias current of about 30 μa. Fig. 13 shows how the voltage sensitivity, the noise and the tangential sensitivity vary with bias current for a typical crystal of this type. The use of forward bias with these crystals is seen to be extremely beneficial.

The theory of low level detection given by Torrey and Whitmer [6] is extended slightly in Appendix III to include the effect of forward bias. The parameter entering into this theory, which cannot be accurately measured, is the barrier capacitance without bias C_0. The theoretical curve for voltage sensitivity vs bias current is brought into close agreement with the experimental curve when it is assumed that $C_0 = 0.023$ pf which is consistent with a contact radius of about 1 micron.

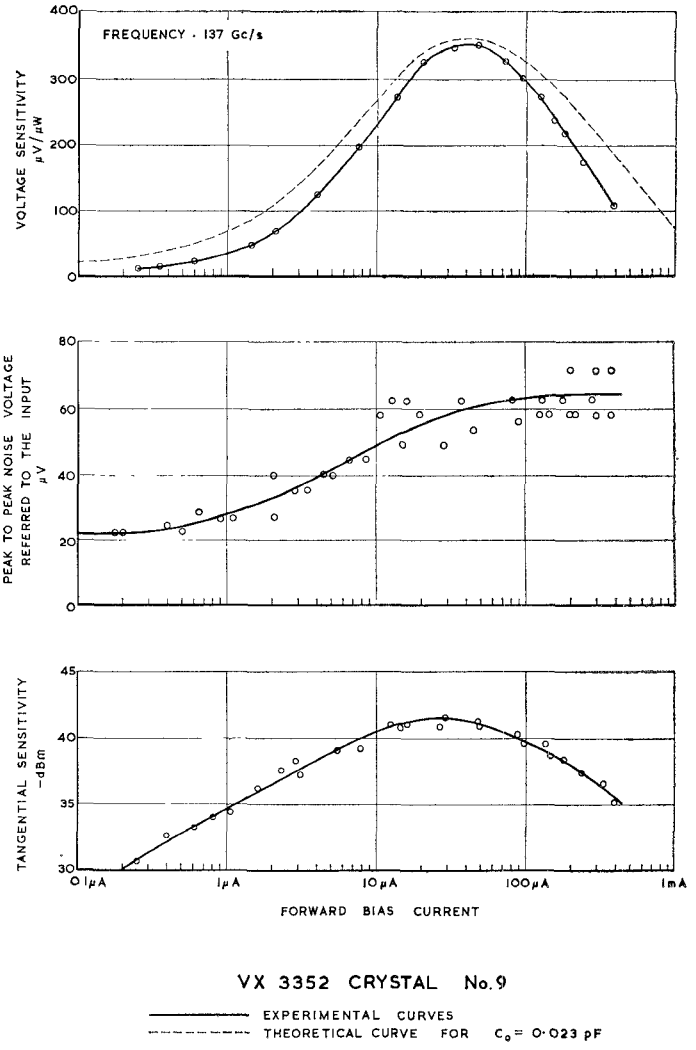

Fig. 13—Performance curves for the 2-mm crystal video receiver.

In a recent series of transmission measurements on ZETA with this new equipment, no receiver noise could be seen on the cathode-ray tube display when everything had been optimized; and the photographs taken when ZETA was fired show, very clearly, the cutoff period followed sometimes by a period of excessive turbulence and, finally, a lengthy interference pattern as the plasma decays (due to multiple reflections inside the torus). Six of these photographs are shown in Fig. 14. In each case, the upper trace shows the ZETA current pulse and the lower trace shows the output from the video amplifier. The cutoff, turbulent and decay periods can easily be recognized. One interference pattern which was studied in detail contains 173 fringes. The bottom right-hand

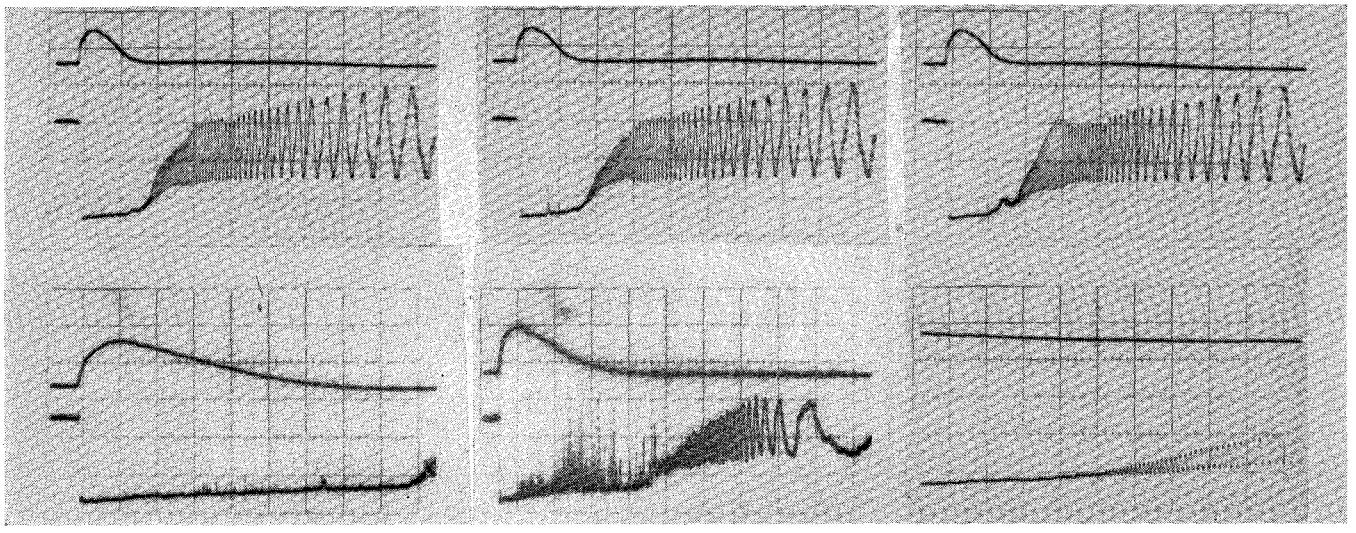

Fig. 14—Photographs of 2-mm transmission through ZETA.

photograph was taken with a faster time base and delayed triggering and it shows the gradual build up of the interference pattern.

Possible Ways of Improving the Performance of Millimeter Wave Superheterodyne Radiometers

In a superheterodyne radiometer the IF amplifier should be designed to have the highest possible value for $\sqrt{\text{bandwidth}}/\text{noise}$ factor. The 70-Gc radiometer described earlier contains a conventional valve IF amplifier with a bandwidth of 10 Mc and a noise factor of 2 db. Thus, expressing the bandwidth, B, in Mc and the noise factor, F_{IF}, as a power ratio, it is seen that the $\sqrt{B}/F_{IF}$ value for this amplifier is 2. In the new 140-Gc radiometer, which has an Adler tube in the first IF stage, the $\sqrt{B}/F_{IF}$ value is 4. A very much higher $\sqrt{B}/F_{IF}$ value than this could be obtained by using a low noise traveling-wave tube in the first IF stage and further traveling-wave tubes of the same bandwidth throughout the rest of the IF amplifier. At the present time it is possible to obtain a low noise S band traveling-wave amplifier with a bandwidth of 2 Gc and a noise factor of 4.3 db. A tube of this type has a $\sqrt{B}/F_{IF}$ value of 16.6 and would therefore give an improvement of more than 4 times compared with the IF amplifier used in our latest radiometer. This factor would only be gained if the output bandwidth of the balanced mixer could be made as large as that of the traveling-wave tubes. Some thought has been given to this problem at R.R.E. and it appears to be capable of solution.

A further improvement in radiometer performance would be obtained if the spreading resistance of mixer crystals could be reduced. With this objective in mind, Messenger [24] proposed the use of a semiconductor wafer thin compared with the contact radius and he suggested the use of jet etching and microalloying techniques to obtain the required structure. This approach has not been pursued seriously in Britain, but the Associated Electrical Industries (A.E.I., Ltd.) are endeavoring at present to achieve the same objective by using epitaxial techniques. Some of the epitaxial silicon which they have produced recently gives significantly better results at millimeter wavelengths than it is possible to obtain with ordinary silicon, but it is not quite up to germanium standard yet.

Further improvements in mixer crystal performance may result from the use of certain III–V compounds. Greatly improved performance is expected from gallium arsenide (see Fig. 1). The small amount of work carried out at R.R.E. on GaAs did not yield any results superior to those obtainable with germanium, but Sharpless [25] has reported outstanding results with GaAs at 55 Gc so the use of this material is one of the bright hopes for the future. The electron mobilities in indium antimonide and indium arsenide are considerably higher than in gallium arsenide [24], but these materials have low energy gaps and are only expected to give good results when cooled. Early work on indium antimonide mixer crystals at R.R.E. has been rather disappointing.

Comparison of the Sensitivities of the Various Types of Detectors Which Are Now Available for Use at Short Millimeter Wavelengths

With infrared-type detectors and the crystal video radiometer, the minimum detectable temperature change is given by [26]

$$\Delta T = \frac{K\sqrt{B_{out}}}{kB_{in}} \tag{1}$$

where K is the minimum detectable change in power with a 1-cps output bandwidth, k is Boltzmann's constant and B_{in} and B_{out} are the input and output bandwidths, respectively.

For a superheterodyne radiometer the corresponding equation is [12]

$$\Delta T = \frac{\pi F T_0}{2}\sqrt{\frac{B_{out}}{B_{IF}}} \tag{2}$$

TABLE I

COMPARISON OF DETECTORS AT A WAVELENGTH OF 2 MM

Type of Detector	Minimum Detectable Power When $B_{out}=1$ cps	Noise Factor	Input Bandwidth	Minimum Detectable Temperature Change When $B_{out}=1$ cps
Golay cell[27]	2×10^{-10} W	—	15 Gc*	960°C
Evacuated barretter[26]	4×10^{-11} W	—	15 Gc*	190°C
Crystal video radiometer with a forward biased VX 3352	2.5×10^{-11} W	—	15 Gc*	120°C
1.5°K carbon bolometer[28]	10^{-11} W	—	15 Gc*	48°C
Present harmonic mixer radiometer	1.3×10^{-14} W	25 db	2×10 Mc	46°C
Existing superheterodyne radiometer with fundamental mixing	7×10^{-15} W	20 db	2×30 Mc	8.3°C
1.5°K InSb photoconductive detector[2],[3]	10^{-12} W	—	15 Gc*	4.8°C

* Restricted to 10 per cent to obtain adequate frequency resolution.

where F is the over-all noise factor T_0 is room temperature and B_{IF} is the IF bandwidth.

Using (1) and (2) and results accumulated during recent years mainly at R.R.E., Table I has been compiled. This compares the performances of seven different types of detectors which are now available for use at a wavelength of 2 mm.

Fig. 15 shows how the performances of the better detectors vary over the wavelength range 4 to 1 mm. The four curves for crystal mixer superheterodyne radiometers are rising at a rate of 6 db per octave throughout this region due to the presence of spreading resistance and barrier capacitance in the mixer crystals. When calculating these four curves, fundamental mixing in germanium diodes was assumed. The curve for the Putley InSb photoconductive detector was calculated for an input bandwidth of 10 per cent because plasma physicists and radio astronomers usually require a fair amount of frequency resolution in their measurements.

With the assumptions made, it is seen that superheterodyne radiometers give a better performance than the Putley detector at a wavelength of 4 mm, the crossover occurs somewhere in the region of 2 mm and at 1 mm the Putley detector is more sensitive than the best superheterodyne radiometer which could be made with currently available components.

Before concluding this section two possible ways of obtaining greatly improved radiometer performance will be mentioned. It is reported[1] that a very broad-band low-noise 4-mm traveling-wave amplifier is now under development with the following target specification: bandwidth 30 Gc, noise factor 10 db, gain 25 db. If this objective is achieved, it would be possible to make a straight traveling-wave tube radiometer which would be about seven times more sensitive than the best superheterodyne radiometer that it appears to be possible to make at this wavelength.

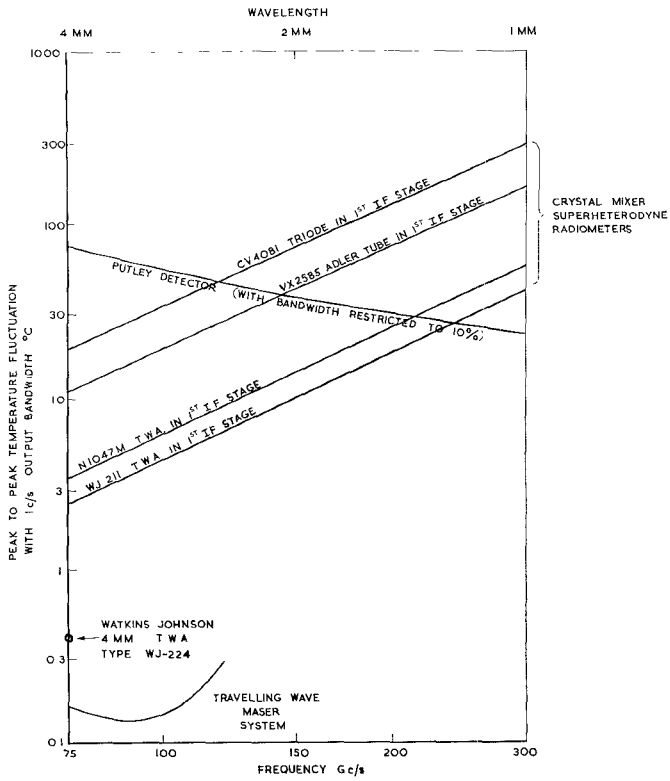

Fig. 15—Theoretical curves of peak-to-peak temperature fluctuations vs frequency for various types of radiometers.

However, even better performance than this now seems to be realizable. Since considerable pump power can now be obtained at short millimeter wavelengths, the development of a 4-mm traveling-wave maser has now become a distinct possibility. If a bandwidth of 400 Mc could be achieved—a value which the experts believe to be possible—then the radiometer performance with an upward looking aerial would be as indicated by

[1] Tentative specification for the Watkin's Johnson traveling-wave amplifier type WJ-224.

the bottom curve in Fig. 15. The main source of noise would now be radiation from the earth's atmosphere and best performance would be obtained in the region of 80 to 90 Gc where the atmospheric attenuation has its lowest value in the V-band window. With this tremendous sensitivity and an aerial gain of about 70 db, temperature measurements could be made on all the planets except Neptune and Pluto.

Conclusions

Superheterodyne receiver techniques have been successfully extended up to a frequency of 140 Gc. Extension of conventional techniques to even higher frequencies would not appear to be profitable for radiometer applications, as the sensitivity would become inferior to that obtainable with existing Putley InSb photoconductive detectors. However, the minimum power which a superheterodyne receiver will detect gets less and less as the input bandwidth is reduced; so, in narrow-band applications with coherent signals, a superheterodyne receiver is capable, even at short millimeter wavelengths, of detecting powers several orders of magnitude lower than the minimum power which can be detected with an infrared type of receiver.

A tremendous advantage of the Putley detector in plasma diagnostic work is that it can be tuned over two decades (0.1 mm to 1 cm) by simply rotating gratings. Perhaps the greatest advantage of the superheterodyne radiometer is that it operates at room temperature whereas the Putley detector must be cooled down to liquid helium temperature.

Our work on mixer and detector crystals has shown that germanium gives better results than silicon at short millimeter wavelengths. Our failure to achieve better results with GaAs than Ge is attributed solely to the fact that, in Britain, very little work has been done so far on point contact GaAs diodes.

The theoretical curve for silicon in Fig. 1 seems to be fairly accurate but the curve for germanium is rather optimistic. In the case of germanium diodes, the values deduced for the zero-bias barrier capacitance from millimeter wave measurements are lower than the theoretical value obtained in Appendix I, while the measured values for the spreading resistance are higher than the corresponding theoretical value. To bring the experimental and theoretical values into closer agreement, it seems to be necessary to assume that the contact radius achieved in the latest germanium millimeter wave diodes is even lower than the value of 1.25 microns which was used in the calculations reported in Appendix I. Photographs of the actual contacts taken through a powerful microscope do not confirm this; so one is forced to the conclusion that only part of the area under the whisker point is in electrical contact with the germanium. The barrier capacitance values needed to account for mixer performance are 2 to 3 times higher than the zero bias values. Two of the reasons for this are given below.

1) In all cases where germanium diodes were employed as mixers or harmonic mixers, forward bias was used as this was found to give a slight improvement in the over-all noise factor, due to a reduction in the noise temperature ratio [30], but (23) shows that this bias causes an increase in the barrier capacitance.
2) Under mixing conditions, particularly with forward bias from a low impedance source, it follows from integration of (23) that the local oscillator voltage will cause a further increase in the mean value of the barrier capacitance (averaged over a complete local oscillator cycle), and this is the value which must be used in (3).

With silicon mixer crystals, forward bias produces no beneficial effect and is not used, so the simple theory in Appendix I is more applicable to silicon than germanium. The theoretical values obtained for the spreading resistance and barrier capacitance with silicon are in reasonable agreement with the values of 50 ohms and 0.05 pf reported by Shurmer [31] for the type VX 4150 Ka-band silicon detector crystal.

The performance obtained from the 140-Gc radiometer with harmonic mixing was quite gratifying and it is felt that harmonic mixing is worthy of serious consideration for narrow-band applications at submillimeter wavelengths.

Although the crystal video receiver is about 25 times less sensitive than the Putley detector at a wavelength of 2 mm, its advantages are: very low cost, extreme simplicity, small size and weight, a response time of a few nanoseconds if needed, and, perhaps most important of all, it does not have to be cooled down to liquid helium temperature. Since plenty of transmitter power can now be obtained at short millimeter wavelengths, it is felt that crystal video receivers will be widely used in future plasma transmission measurements at all wavelengths down to about 1 mm.

Appendix I

The Theoretical Performance of Mixer Crystals in the Millimeter and Submillimeter Regions

Sharpless [8] has shown that the over-all noise factor at an angular frequency, ω, is given by

$$F = L_0\{F_{IF} + t - 1\}\frac{r + \dfrac{R}{1 + (\omega CR)^2}}{\dfrac{R}{1 + (\omega CR)^2}} \qquad (3)$$

where L_0 is the conversion loss with zero spreading resistance, F_{IF} is the IF noise factor, t is the noise temperature ratio of the crystal, r is the spreading resistance, C is the barrier capacitance and R is the barrier input resistance at the signal frequency.

TABLE II

	P-Type Silicon	N-Type Germanium	N-Type Gallium Arsenide
Optimum carrier density, N	5×10^{18} per cm^3	2×10^{18} per cm^3	2×10^{17} per cm^3
Mobility, b	70 $\frac{\text{cm}^2}{\text{volt-sec}}$	800 $\frac{\text{cm}^2}{\text{volt-sec}}$	4500 $\frac{\text{cm}^2}{\text{volt-sec}}$
Resistivity $\rho=\frac{1}{Nqb}$	0.018 ohm-cm	0.004 ohm-cm	0.007 ohm-cm
Spreading resistance $r=\frac{\rho}{4a}$	36 ohms	8 ohms	14 ohms
Dielectric constant, ϵ	12	16	11
Barrier height ϕ	0.3 volt	0.3 volt	0.8 volt
Barrier capacitance $C=\pi a^2\left\{\frac{\epsilon\epsilon_0 Nq}{2\phi}\right\}^{1/2}$	0.059 pf	0.043 pf	0.007 pf

Note: q is the electronic charge, 1.6×10^{-19} coulombs, and $\epsilon_0=\frac{1}{36\pi\times10^9}$.

The curves shown in Fig. 1 are based upon this equation. The standard expressions for barrier capacitance and spreading resistance [6] and the optimum values for carrier concentrations [9], [10] were used. The lowest value for the contact radius, a reported in the literature appears to be 1.25×10^{-4} cm [8]; so this value was used for each material. It was assumed that the capacitance which affects mixer crystal operation is equal to the zero-bias capacitance, but this point is discussed further in the Conclusions. The values obtained for C and r are given in Table II. The other constants used in the calculations, and not shown in Fig. 1, were $L_0=4.2$ db and $R=180$ ohms. These were obtained from the curves given by Southworth [7] for $n=5$ and $R_{IF}=300$ ohms, which appear to be typical practical values for each material. (R_{IF} denotes the IF impedance and n is the slope of the log current vs log voltage curve for the forward characteristic of the diode.)

Appendix II

Theory of Second Harmonic Mixing

In most of this analysis the spreading resistance and barrier capacitance are completely neglected.

Let the current voltage characteristic of the harmonic mixer diode be represented by the following equation:

$$i = A\{\epsilon^{\alpha e} - 1\}. \tag{4}$$

The instantaneous conductance of this diode is then given by

$$g = \frac{di}{de} = \alpha A \epsilon^{\alpha e}. \tag{5}$$

Let $e=e_1\cos\omega_c t$, where e_1 is the peak value of the local oscillator voltage and ω_c is the angular frequency of the local oscillator. Then

$$\begin{aligned} g &= \alpha A \epsilon^{\alpha e_1\cos\omega_c t} \\ &= \alpha A\{I_0(\alpha e_1) + 2I_1(\alpha e_1)\cos\omega_c t + 2I_2(\alpha e_1)\cos 2\omega_c t \\ &\quad + 2I_3(\alpha e_1)\cos 3\omega_c t + \cdots\} \end{aligned} \tag{6}$$

where $I_0(\alpha e_1)$, $I_1(\alpha e_1)$, etc., are modified Bessel functions with argument (αe_1). $[I_n(x)=j^{-n}J_n(jx)]$. The first five terms in (6) are needed in this analysis and, for simplicity, (6) will be rewritten as

$$\begin{aligned} g &= g_0 + 2g_1\cos\omega_c t + 2g_2\cos 2\omega_c t + 2g_3\cos 3\omega_c t \\ &\quad + 2g_4\cos 4\omega_c t \end{aligned} \tag{7}$$

where

$$g_0 = \alpha A I_0(\alpha e_1), \qquad g_1 = \alpha A I_1(\alpha e_1), \text{ etc.} \tag{8}$$

Following Southworth [7], the harmonic mixer can now be represented by the equivalent circuit shown in Fig. 16.

Let the currents flowing round this equivalent circuit at the signal, image and intermediate frequencies be denoted, respectively, by $i_S\cos\omega_S t$, $i_i\cos\omega_i t$ and $i_{IF}\cos\omega_{IF} t$.

For second harmonic mixing (with the second harmonic of the local oscillator on the low side of the signal frequency) we have

$$\omega_S = 2\omega_c + \omega_{IF} \tag{9}$$

$$\omega_i = 2\omega_c - \omega_{IF}. \tag{10}$$

The voltage appearing across the harmonic mixer diode is seen from Fig. 16 to be

$$\begin{aligned} v &= e_S\cos\omega_S t - i_S R_S\cos\omega_S t - i_i R_S\cos\omega_i t \\ &\quad - e_{IF}\cos\omega_{IF} t \end{aligned} \tag{11}$$

and

$$\begin{aligned} vg &= i_S\cos\omega_S t + i_i\cos\omega_i t + i_{IF}\cos\omega_{IF} t \\ &\quad + \text{other terms of no interest in this present analysis.} \end{aligned} \tag{12}$$

After substituting (7) and (11) into (12) and equating the coefficients of $\cos\omega_S t$, $\cos\omega_i t$ and $\cos\omega_{IF} t$, we get, in matrix form,

$$\begin{bmatrix} i_S \\ i_{IF} \\ i_i \end{bmatrix} = \begin{bmatrix} g_0 & g_2 & g_4 \\ g_2 & g_0 & g_2 \\ g_4 & g_2 & g_0 \end{bmatrix} \begin{bmatrix} e_S - i_S R_S \\ -e_{IF} \\ -i_i R_S \end{bmatrix}. \tag{13}$$

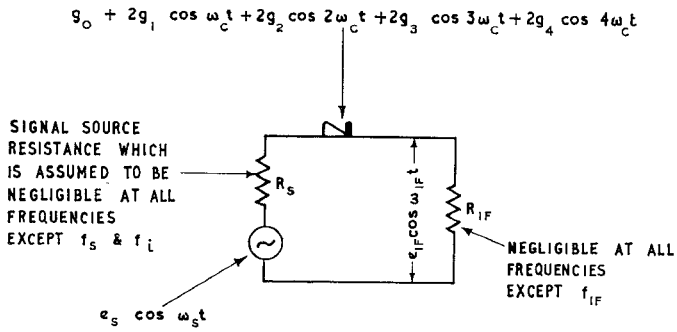

Fig. 16—Equivalent circuit of harmonic mixer crystal.

Proceeding now along the same lines that Torrey and Whitmer [6] followed, when working out their theory of fundamental mixing, it is found that the conversion loss for second harmonic mixing is given by

$$L = \frac{R_S\left(g_0+g_4+\frac{1}{R_S}\right)\left[g_0\left(g_0+g_4+\frac{1}{R_S}\right)-2(g_2)^2\right]}{(g_2)^2}. \quad (14)$$

On differentiating (14) with respect to R_S and equating to zero, it is found that the second harmonic conversion loss has a minimum value when

$$R_S = \frac{1}{(g_0 + g_4)\sqrt{1-\eta}} = \frac{1}{\alpha A\{I_0(\alpha e_1) + I_4(\alpha e_1)\}\sqrt{1-\eta}} \quad (15)$$

where

$$\eta = \frac{2(g_2)^2}{g_0(g_0+g_4)} = \frac{2\{I_2(\alpha e_1)\}^2}{I_0(\alpha e_1)\{I_0(\alpha e_1) + I_4(\alpha e_1)\}}. \quad (16)$$

When (15) is satisfied, the second harmonic conversion loss is given by

$$L_{\min} = 2\frac{1+\sqrt{1-\eta}}{1-\sqrt{1-\eta}}. \quad (17)$$

The input resistance of the harmonic mixer at the signal frequency is equal to the value of R_S which gives minimum second harmonic conversion loss; so it is also given by (15).

The curves for second harmonic mixing shown in Fig. 9 were calculated from (15), (16) and (17), using the tables of modified Bessel functions given by Wrinch and Wrinch [29].

The rectified crystal current for both fundamental and second harmonic mixing is given by

$$i_m = \frac{\int_{t=0}^{t=2\pi/\omega} A\{\epsilon^{\alpha e_1 \cos \omega_c t} - 1\}\,dt}{\frac{2\pi}{\omega}} = A\{I_0(\alpha e_1) - 1\}. \quad (18)$$

The noise temperature ratio, t, of the diode is linearly related to the crystal current; so we can write

$$t = 1 + Ki_m \quad (19)$$

where K is a constant whose value is unity for the curve in Fig. 9 and 1.6 for the curve in Fig. 10, with i_m expressed in ma.

The curve in Fig. 10 giving the loss due to spreading resistance and barrier capacitance was calculated using the last factor in (3).

Appendix III

Voltage Sensitivity of a Forward Biased Detector Crystal

Assume that the forward bias current, I, and the voltage across the barrier, V, are related by the usual equation,

$$I = A\{\epsilon^{\alpha V} - 1\}. \quad (20)$$

Using the microwave equivalent circuit shown in Fig. 17, Torrey and Whitmer [6] have shown that the current sensitivity of a detector crystal, at an angular frequency ω, is given by

$$\beta = \frac{\alpha}{2\left(1+\frac{r}{R}\right)^2}\frac{1}{\left(1+\frac{\omega^2C^2rR^2}{R+r}\right)}. \quad (21)$$

When the following video amplifier has an input resistance, R_{in}, the equivalent input circuit, for low video frequencies, is as shown in Fig. 18, where P represents the absorbed RF power. The voltage sensitivity is then given by

$$S = \frac{e}{P} = \frac{\alpha}{2}\frac{R_{\text{in}}}{(R+r+R_{\text{in}})}\cdot\frac{R^2}{(R+r+\omega^2C^2rR^2)}. \quad (22)$$

Denoting the zero-bias capacitance by C_0 and the barrier height by ϕ, Torrey and Whitmer [6] have shown that

$$C = \frac{C_0}{\sqrt{\left(1-\frac{V}{\phi}\right)}}. \quad (23)$$

Rearranging (20), we get

$$V = \frac{1}{\alpha}\log_\epsilon\frac{I+A}{A}. \quad (24)$$

The slope resistance,

$$R = \frac{dV}{dI} = \frac{1}{\alpha(I+A)}. \quad (25)$$

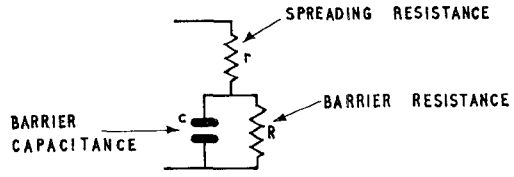

Fig. 17—Microwave equivalent circuit of detector crystal.

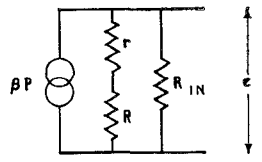

Fig. 18—Equivalent input circuit for low video frequencies.

From (22), (23), (24) and (25) we get

$$S = \frac{\alpha}{2} \frac{R_{\text{in}}}{\left\{\frac{1}{\alpha(I+A)} + r + R_{\text{in}}\right\}} \frac{\frac{1}{\alpha^2(I+A)^2}}{\left\{\frac{1}{\alpha(I+A)} + r + \frac{\omega^2 C_0^2 r}{\left(1 - \frac{1}{\alpha\phi}\log_e \frac{I+A}{A}\right)\alpha^2(I+A)^2}\right\}}. \tag{26}$$

An analysis of the dc characteristic for VX 3352 crystal no. 9 yielded the following values: $A = 0.2$ μa, $\alpha = 22$ volts^{-1}, $r = 24$ Ω and $\phi = 0.45$ volt; and the measured value for R_{in} was 3 kΩ. The only remaining unknown now is C_0 and (26) gives a theoretical curve, for 140 Gc, in close agreement with the experimental curve for this particular crystal when it is assumed that $C_0 = 0.023$ pf (see Fig. 13).

Acknowledgment

The authors wish to thank all of their colleagues in R.R.E. Millimetre Wave Division, R.R.E. Engineering Department and the ZETA team at Harwell for their very considerable help in all of the work which has been described. Grateful thanks are also extended to A.E.I. Ltd., General Electric Company, Ltd., and the Services Electronics Research Laboratory who have supplied the authors with the semiconductor materials which have been used. Finally, the authors would like to thank the United Kingdom Atomic Energy Authority for supporting all of this work and the Ministry of Aviation for permission to publish this paper.

References

[1] P. C. Thonemann, *et al.*, "Production of high temperatures and nuclear reactions in a gas discharge," *Nature*, vol. 181, pp. 217–220; January 25, 1958.
[2] E. H. Putley, "Impurity photoconductivity in N-type InSb," *Proc. Phys. Soc.*, vol. 76, pp. 802–805; November, 1960.
[3] ——, "Impurity photoconductivity in N-type InSb," *J. Phys. Chem. Solids*, vol. 22, pp. 241–247; 1961.
[4] G. N. Harding, *et al.*, "Emission of sub-millimetre electromagnetic radiation from hot plasma in Zeta," *Proc. Phys. Soc.*, vol. 77, pp. 1069–1075; 1961.
[5] G. N. Harding and V. Roberts, "Spectroscopic Investigation of Plasma in the Wavelength Range 0.1–2.0 mm," *Proc. 5th Internat'l. Conf. on Ionization Phenomena in Gases*, pp. 1977–1986; 1961.
[6] H. C. Torrey and C. A. Whitmer, "Crystal Rectifiers," McGraw-Hill Book Company, Inc., New York, N. Y., chs. 4, 5 and 11; 1948.
[7] G. C. Southworth, "Principles and Applications of Waveguide Transmission," D. Van Nostrand Co., Inc., Princeton, N. J., ch. 12; 1950.
[8] W. M. Sharpless, "Wafer type millimetre wave rectifiers," *Bell Sys. Tech. J.*, vol. 35, pp. 1385–1402; November, 1956.
[9] G. C. Messenger and C. T. McCoy, "Theory and operation of crystal diodes as mixers," Proc. IRE, vol. 45, pp. 1269–1283; September, 1957.
[10] D. A. Jenny, "A gallium arsenide microwave diode," Proc. IRE, vol. 46, pp. 717–722; April, 1958.
[11] B. B. van Iperen, "Reflex klystrons for wavelengths of 4 and 2.5 mm," *Philips Tech. Rev.*, vol. 21, pp. 221–228; June, 1960.
[12] R. H. Dicke, "The measurement of thermal radiation at microwave frequencies," *Rev. Sci. Instr.*, vol. 17, pp. 268–275; July, 1946.
[13] E. F. Grant, "An analysis of the sensing method of automatic frequency control for microwave oscillators," Proc. IRE, vol. 37, pp. 943–951; August, 1949.
[14] C. R. Ditchfield, "Crystal mixer design at frequencies from 20,000 to 60,000 Mc/s," *Proc. IEE*, vol. 100, pt. 3, pp. 365–371; November, 1953.
[15] R. Meredith and G. H. Preece, "A Range of 2 and 1 Millimetre Waveguide Components," presented at the IEEE Millimeter and Submillimeter Conf., Orlando, Fla.; January 8–10, 1963.
[16] D. J. H. Wort, "Solar temperature at 2 mm wavelength," *Nature*, vol. 195, pp. 1288–1289; September 29, 1962.
[17] F. M. Colebrook and G. H. Aston, "Diode as a frequency changer," *Wireless Eng.*, vol. 20, pp. 5–14; January, 1943.
[18] C. M. Johnson, "Superheterodyne receiver for the 100 to 150 kMc region," IRE Trans. on Microwave Theory and Techniques, vol. MTT-2, pp. 27–32; September, 1954.
[19] G. S. Heller, "Millimeter instrumentation for solid state research," *Proc. Symp. on Millimeter Waves*, Polytechnic Press of the Polytechnic Institute of Brooklyn, N. Y., pp. 73–85; 1960.
[20] G. Convert, "Sub-Millimetre Wave Generation using Conventional Means," presented at the C.V.D. Symp. on Millimetre Wave Generation, Sheffield University, England; September, 1961.
[21] R. Adler, G. Hrbek, and G. Wade, "A low-noise electron-beam parametric amplifier," Proc. IRE (*Correspondence*), vol. 46, pp. 1756–1757; October, 1958.
[22] ——, "The quadrupole amplifier, a low-noise parametric device," Proc. IRE, vol. 47, pp. 1713–1723; October, 1959.
[23] R. W. White and R. Hamer, "A Series Compensated Tuned Intervalve Coupling Circuit," Post Office Engineering Dept., Radio Rept. No. 2212; 1952.
[24] G. C. Messenger, "New concepts in microwave mixer diodes," Proc. IRE, vol. 46, pp. 1116–1121; June, 1958.
[25] W. M. Sharpless, "High frequency gallium arsenide point-contact rectifiers," *Bell Sys. Tech. J.*, vol. 38, pp. 259–269; January, 1959.
[26] M. W. Long and W. K. Rivers, Jr., "Submillimeter wave radiometry," Proc. IRE, vol. 49, pp. 1024–1027; June, 1961.
[27] M. J. E. Golay, "A pneumatic infra-red detector," *Rev. Sci. Instr.*, vol. 18, pp. 357–362; May, 1947.
[28] W. S. Boyle and K. F. Rodgers, "Performance characteristics of a new low-temperature bolometer," *J. Opt. Soc. Am.*, vol. 49, pp. 66–69; January, 1959.
[29] H. E. H. Wrinch and D. Wrinch, "Tables of the Bessel function $I_n(x)$," *Philosophical Magazine*, vol. 45, pp. 846–849; 1923; and vol. 47, pp. 62–65; 1924.
[30] A. Lindell and T. Oxley, "Radar crystal valves," *Proc. IEE*, vol. 106, pt. B, suppl. no. 15, pp. 426–433; 1959.
[31] H. V. Shurmer, "Crystal detectors to cover the frequency band 26–40 Gc/s," *Proc. IEE*, vol. 108, pt. B, pp. 659–665; November, 1961.